Research paper

Leaf morphological and physiological adaptations of a deciduous oak (*Quercus faginea* Lam.) to the Mediterranean climate: a comparison with a closely related temperate species (*Quercus robur* L.)

José Javier Peguero-Pina[1,†], Sergio Sisó[1,†], Domingo Sancho-Knapik[1], Antonio Díaz-Espejo[2], Jaume Flexas[3], Jeroni Galmés[3] and Eustaquio Gil-Pelegrín[1,4]

[1]Unidad de Recursos Forestales, Centro de Investigación y Tecnología Agroalimentaria, Gobierno de Aragón, Avenida Montañana 930, 50059 Zaragoza, Spain; [2]Irrigation and Crop Ecophysiology Group, Instituto de Recursos Naturales y Agrobiología de Sevilla (IRNAS, CSIC), Avenida Reina Mercedes 10, 41012 Sevilla, Spain; [3]Research Group on Plant Biology under Mediterranean Conditions, Departament de Biologia, Universitat de les Illes Balears, Carretera de Valldemossa, 07071 Palma de Mallorca, Spain; [4]Corresponding author (egilp@aragon.es)

'White oaks'—one of the main groups of the genus *Quercus* L.—are represented in western Eurasia by the 'roburoid oaks', a deciduous and closely related genetic group that should have an Arcto-Tertiary origin under temperate-nemoral climates. Nowadays, roburoid oak species such as *Quercus robur* L. are still present in these temperate climates in Europe, but others are also present in southern Europe under Mediterranean-type climates, such as *Quercus faginea* Lam. We hypothesize the existence of a coordinated functional response at the whole-shoot scale in *Q. faginea* under Mediterranean conditions to adapt to more xeric habitats. The results reveal a clear morphological and physiological segregation between *Q. robur* and *Q. faginea*, which constitute two very contrasting functional types in response to climate dryness. The most outstanding divergence between the two species is the reduction in transpiring area in *Q. faginea*, which is the main trait imposed by the water deficit in Mediterranean-type climates. The reduction in leaf area ratio in *Q. faginea* should have a negative effect on carbon gain that is partially counteracted by a higher inherent photosynthetic ability of *Q. faginea* when compared with *Q. robur*, as a consequence of higher mesophyll conductance, higher maximum velocity of carboxylation and much higher stomatal conductance (g_s). The extremely high g_s of *Q. faginea* counteracts the expected reduction in g_s imposed by the stomatal sensitivity to vapor pressure deficit, allowing this species to diminish water losses maintaining high net CO_2 assimilation values along the vegetative period under nonlimiting soil water potential values. In conclusion, the present study demonstrates that *Q. faginea* can be regarded as an example of adaptation of a deciduous oak to Mediterranean-type climates.

Keywords: leaf area, roburoid oaks, stomatal conductance, vapor pressure deficit.

Introduction

The genus *Quercus* L. (Fagaceae) comprises ~400 tree and shrub species distributed among contrasting phytoclimates in the Northern Hemisphere, from temperate and subtropical deciduous forests to Mediterranean evergreen woodlands (Manos et al. 1999, Kremer et al. 2012). Although the successive infrageneric classifications of *Quercus* have undergone changes, all of them recognized the same major groups (see

[†]These authors contributed equally to this study.

Denk and Grimm 2010 and references therein). One of the main groups is the so-called 'Group *Quercus*' or 'white oaks' (Denk and Grimm 2009), which is represented in western Eurasia by the so-called 'roburoid oaks' (Denk and Grimm 2010). The roburoid oaks that should have their origin in Arcto-Tertiary lineages during the Early Tertiary (Axelrod 1983, Kovar-Eder et al. 1996) are a quite coherent group of species with a high degree of genetic similarity (Olalde et al. 2002, Denk and Grimm 2010). Nowadays, one of the greatest representative roburoid oak species widely distributed along a temperate-nemoral climate is *Quercus robur* L., which is considered a meso-hygrophilous species (Piedallu et al. 2013) distributed in Europe from Spain to southern Scandinavia and from Ireland to eastern Europe (Ducousso and Bordacs 2004).

Nevertheless, the roburoid oaks are not exclusive of the temperate climates, but they are also present in southern Europe under Mediterranean-type climates (Corcuera et al. 2004, Himrane et al. 2004, Sánchez de Dios et al. 2009), which evidences the ability to survive in more xeric habitats (Kvacek and Walther 1989, Barrón et al. 2010). This may be the case of *Quercus faginea* Lam., for which the first fossil records, found in the south of France, coincide with the development of the Mediterranean seasonality during the Pliocene (Roiron 1983, Barrón et al. 2010).

Quercus faginea is the most abundant and widely distributed white oak in the Iberian Peninsula (Olalde et al. 2002). Some previous studies that have dealt with the resistance to drought of this species are mainly based on the comparison with other Mediterranean oak species, such as the evergreen *Quercus ilex* (Corcuera et al. 2002, Mediavilla and Escudero 2003). This comparison makes sense in terms of forest composition and vegetation dynamic in most continental Mediterranean areas of the Iberian Peninsula (Mediavilla and Escudero 2004), where *Q. faginea* and *Q. ilex* co-occur. These congeneric species constitute two examples of contrasting leaf habit, which itself represents quite different functional strategies (Kikuzawa 1995). In this sense, it has been proposed that the evergreen condition of *Q. ilex* would allow this species to assimilate carbon throughout a longer time period (Acherar and Rambal 1992, Ogaya and Peñuelas 2007, van Ommen Kloeke et al. 2012), which was empirically confirmed in cold Mediterranean areas (Corcuera et al. 2005a). On the contrary, the leaf life span of the deciduous *Q. faginea* limits the photosynthetic activity to a shorter period, implying the need for higher rates of carbon gain under favorable conditions (van Ommen Kloeke et al. 2012).

However, the importance in the Mediterranean forest landscape of the Iberian Peninsula and north of Africa of such deciduous Mediterranean oaks, such as *Q. faginea* and other congeneric species (Olalde et al. 2002, Benito Garzón et al. 2007, Sánchez de Dios et al. 2009), indicates that this leaf habit performs adequately under the limiting climatic conditions of Mediterranean areas. Therefore, some roburoid oaks, such as *Q. faginea*, must have developed functional strategies to adapt to the summer drought conditions, withstanding both edaphic and atmospheric water stresses.

In order to evaluate the physiological traits that *Q. faginea* shows for coping with the Mediterranean aridity, we established an interspecific comparison with *Q. robur*, other roburoid deciduous oak from temperate-nemoral climates. We hypothesize the existence of a coordinated functional response at the whole-shoot scale in *Q. faginea* under Mediterranean conditions. In this sense, the specific objectives of this study are (i) to analyze the morphological, anatomical, hydraulic, photosynthetic and biochemical traits of *Q. faginea* and (ii) to compare them with those from *Q. robur*, a temperate white oak genetically closely related but occurring under contrasting ecological and climatic conditions (Olalde et al. 2002, Himrane et al. 2004).

Materials and methods

Plant material and experimental conditions

Seeds from *Q. robur* L. ('Galicia' provenance, 42°34′N, 8°33′W, 300 m above sea level, Spain) and *Q. faginea* Lam. ('Alcarria-Serranía de Cuenca' provenance, 40°19′N, 2°15′W, 950 m above sea level, Spain) were sown and cultivated in 2009 under the same conditions (mixture of 80% substrate and 20% perlite in 500 ml containers) inside a transparent greenhouse of alveolar polycarbonate (CITA de Aragón, Zaragoza, Spain) that allowed passing 90% of photosynthetic photon flux density (PPFD; ~1500 mmol photons $m^2 s^{-1}$ at midday, during the experiments) and was equipped with an evaporative cooling system, set for keeping the air temperature inside the greenhouse below 30 °C, while air vapor pressure deficit (VPD) was ~1 kPa through the experiments. Such environmental conditions are close to those recorded during the early growing season (May–June) for both species (Figure 1). Periodical surveys (twice a week) yielded no differences in the time of leaf unfolding between both species when cultivated under the same conditions (data not shown). Jato et al. (2002) also reported the same date for leaf unfolding in co-occurring populations of both species in northwestern Spain. After the first growth cycle, the seedlings were transplanted to containers of 25 l. All plants were irrigated every 2 days. Measurements were performed at the end of June 2012 in fully matured leaves of 4-year-old seedlings for both species.

The distribution ranges of each species have contrasting climatic conditions. *Quercus robur* occurs in sites where annual and summer precipitation (P and P_s, respectively) are higher than in the sites where *Q. faginea* occurs (Table 1). The mean annual and summer temperatures (T and T_s, respectively) are higher for the sites where *Q. faginea* occurs (Table 1). As a consequence, the Martonne aridity index [MAI = $P/(T + 10)$] and the Gaussen index (the number of months in which $P < 2T$, where P is the
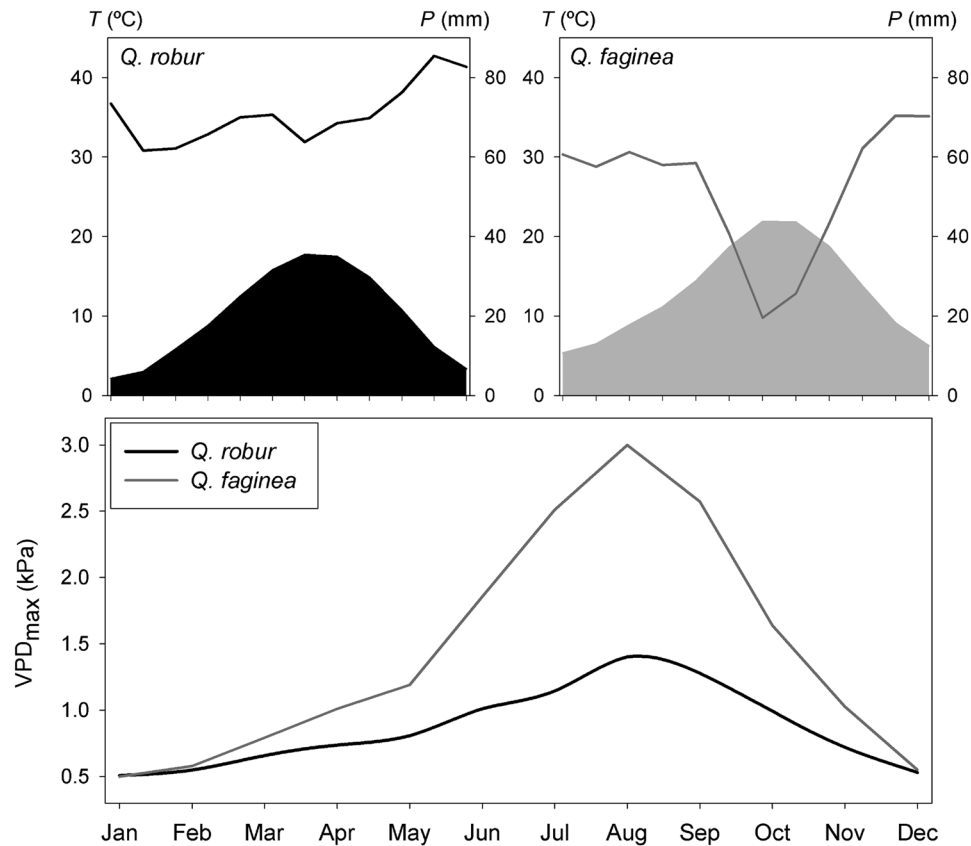
Figure 1. Ombrothermic diagrams showing temperature (T, filled areas) and precipitation (P, lines) (upper panels) and VPD_{max} (lower panel) for the distribution ranges of *Q. robur* and *Q. faginea*.

Table 1. Mean climatic characteristics for the distribution ranges of *Q. robur* and *Q. faginea*: mean annual and summer temperature (T and T_s), total annual and summer precipitation (P and P_s), MAI and Gaussen index. Data are mean ± SE. Different letters indicate statistically significant differences ($P < 0.05$).

Species	T (°C)	T_s (°C)	P (mm)	P_s (mm)	MAI	Gaussen index
Q. robur	9.9 ± 0.3a	17.0 ± 0.2a	850 ± 27a	206 ± 9a	43 ± 2a	0 ± 0a
Q. faginea	13.0 ± 0.3b	20.8 ± 0.3b	628 ± 15b	86 ± 6b	28 ± 1b	2.6 ± 0.2b

monthly precipitation in mm and T is the monthly mean temperature in °C) are also higher for the sites where *Q. faginea* occurs (Table 1, Figure 1). Climatic information was obtained from the WorldClim database (http://www.worldclim.org/) using 70 geographic points throughout the distribution range of *Q. robur* and *Q. faginea*, respectively. Moreover, VPD (kPa) was calculated using the data obtained from WeatherSpark database (http://weatherspark.com/) for six locations of *Q. robur* and *Q. faginea*, respectively. The maximum daily VPD (VPD_{max}, kPa) is much higher for the sites where *Q. faginea* occurs, especially during summer (Figure 1).

Morphological variables

Leaf area and leaf mass area (LMA) were measured in 30 mature leaves sampled from 10 individuals per species (i.e., three leaves were randomly taken from each individual). Leaf area was measured by digitalizing the leaves and using the ImageJ image analysis software (http://rsb.info.nih.gov/nih-image/). Leaves

were then oven-dried at 70 °C for 3 days to determine their dry weight. The LMA was calculated as the ratio of the foliage dry weight to foliage area and was used as an estimator of sclerophylly (Corcuera et al. 2002). Major vein density (MVD) was determined in another set of 10 mature leaves per species following the method described in Scoffoni et al. (2011) with some modifications. Leaves were chemically cleared with 5% NaOH in aqueous solution, washed with bleach solution, dehydrated in an ethanol dilution series (70, 90, 95 and 100%) and stained with safranin. Then, leaves were scanned at 1200 d.p.i. resolution, and the leaf area and lengths of first-, second- and third-order veins were measured using the ImageJ software. Vein densities for each order were calculated as the vein length/leaf area ratio (LAR). The MVD was then obtained as the sum of the first-, second- and third-order vein densities. Finally, the LAR was calculated in 10 current-year shoots per species by dividing the total leaf area per shoot (measured as described above) by the dry weight of the shoot.

Stem hydraulic conductivity

The hydraulic conductivity (K_h, kg m s^{-1} MPa^{-1}) was determined in current-year stem segments of *Q. robur* and *Q. faginea*. Three stem segments (3–5 cm long and >1 mm in diameter) per branch were cut under water from 10 south-exposed branches per species. The measurement pressure was set to 4 kPa. The flow rate was determined with a PC-connected balance (Sartorius BP221S, 0.1 mg precision, Sartorius AG, Göttingen, Germany) by recording the change in weight every 10 s and fitting linear regressions over 200-s intervals. The conductivity measurements were carried out with distilled, filtered (0.22 µm) and degassed water containing 0.005% (volume/volume) Micropur (Katadyn Products, Wallisellen, Switzerland) to prevent microbial growth (Mayr et al. 2006). No native embolism was detected in the segments, as reflected by the comparison of the flow rates before and after applying short perfusions at 0.15 MPa for 60–90 s. The same stem segments were measured in length, diameter without bark and total leaf surface area supplied, to compute the main hydraulic architecture parameters, namely specific conductivity (K_s, kg m^{-1} s^{-1} MPa^{-1}) as the hydraulic conductivity on a sapwood area basis, and leaf-specific conductivity (LSC, kg m^{-1} s^{-1} MPa^{-1}) as hydraulic conductivity on a leaf area basis.

Leaf hydraulic conductance

Leaf hydraulic conductance (K_{leaf}, mmol m^{-2} s^{-1} MPa^{-1}) for *Q. robur* and *Q. faginea* was calculated following the methodology described by Brodribb et al. (2005). Six sun-exposed branches from six plants per species were collected at 07:00–08:00 h (solar time), minimizing the possibility for midday K_{leaf} depression (Brodribb and Holbrook 2004). The branches were enclosed in sealed plastic bags to prevent water loss and stored in the dark for a period of at least 1 h until stomatal closure so that all leaves from the same branch could reach the same water potential. It is assumed that this is the water potential of the leaves prior to rehydration (Ψ_0). Once this value was obtained, one leaf per branch was cut under water to prevent air entry and allowed to take up water for 30–60 s. The water potential after rehydration was subsequently obtained (Ψ_f). The K_{leaf} was calculated according to the following equation:

$$K_{leaf} = \frac{C_l \cdot \ln(\Psi_0/\Psi_f)}{t} \qquad (1)$$

where C_l (mol MPa^{-1} m^{-2}) is the leaf capacitance for each species. C_l was calculated as the initial slope of the pressure–volume relationships, normalized by the leaf area (Brodribb et al. 2005). Pressure–volume relationships for *Q. robur* and *Q. faginea* were determined in six leaves per species, following the free-transpiration method described in previous studies (Vilagrosa et al. 2003).

Leaf gas exchange and chlorophyll fluorescence measurements

Leaf gas exchange parameters were determined simultaneously with measurements of chlorophyll fluorescence using an open gas exchange system (CIRAS-2, PP-Systems, Amesbury, MA, USA) fitted with an automatic universal leaf cuvette (PLC6-U, PP-Systems) with an FMS II portable pulse amplitude modulated fluorometer (Hansatech Instruments Ltd, Norfolk, UK). Six CO_2 response curves were obtained from *Q. robur* and *Q. faginea*. In light-adapted mature leaves, photosynthesis measurements started at a CO_2 concentration surrounding the shoot (C_a) of 400 µmol mol^{-1} and a saturating PPFD of 1500 µmol m^{-2} s^{-1}. Leaf temperature and VPD were maintained at 25 °C and 1.25 kPa, respectively, during measurements. Once a steady-state gas exchange rate was reached under these conditions (usually 30 min after clamping the leaf), net assimilation rate (A_N), transpiration (E), stomatal conductance (g_s) and the effective quantum yield of PSII were estimated. Thereafter, C_a was decreased stepwise down to 50 µmol mol^{-1}. Upon completion of measurements at low C_a, C_a was increased again to 400 µmol mol^{-1} to restore the original value of A_N. Then, C_a was increased stepwise to 1800 µmol mol^{-1}. Leakage of CO_2 in and out of the cuvette was determined for the same range of CO_2 concentrations with a photosynthetically inactive leaf enclosed (obtained by heating the leaf until no variable chlorophyll fluorescence was observed) and used to correct measured leaf fluxes (Flexas et al. 2007*a*).

The effective photochemical efficiency of photosystem II (Φ_{PSII}) was measured simultaneously with A_N and g_s. For Φ_{PSII}, the steady-state fluorescence (F_S) and the maximum fluorescence during a light-saturating pulse of ~8000 µmol m^{-2} s^{-1} (F_M') were estimated, and Φ_{PSII} was calculated as $(F_M' - F_S)/F_M'$, following the procedures of Genty et al. (1989). The photosynthetic electron transport rate (J_{flu}) was then calculated according to Krall and Edwards (1992), multiplying Φ_{PSII} by PPFD and by α (a term that includes the product of leaf absorptance and the partitioning of absorbed quanta between photosystems I and II). α was previously determined for each species as the slope of the relationship between Φ_{PSII} and Φ_{CO_2} (i.e., the quantum efficiency of CO_2 fixation) obtained by varying light intensity under nonphotorespiratory conditions in an atmosphere containing <1% O_2 (Valentini et al. 1995). Five light curves from *Q. robur* and *Q. faginea* were measured to determine α.

Estimation of mesophyll conductance by gas exchange and chlorophyll fluorescence

Mesophyll conductance (g_m) was estimated according to the method of Harley et al. (1992), as follows:

$$g_m = \frac{A_N}{C_i - [\Gamma^* (J_F + 8(A_N + R_L))/J_F - 4(A_N + R_L)]} \qquad (2)$$

where A_N and the substomatal CO_2 concentration (C_i) were taken from gas exchange measurements at saturating light, whereas Γ^* (the chloroplastic CO_2 photocompensation point in the absence of mitochondrial respiration) and R_L (the respiration rate in the light) were estimated for each species according to the Laisk (1977) method, following the methodology

described in Flexas et al. (2007b). The values of g_m obtained were used to convert $A_N–C_i$ into $A_N–C_c$ curves (where C_c is the chloroplastic CO_2 concentration) using the equation $C_c = C_i – A_N/g_m$. The maximum carboxylation and J_{flu} capacities ($V_{c,max}$ and J_{max}, respectively) were calculated from the $A_N–C_c$ curves, using the Rubisco kinetic constants and their temperature dependence described by Bernacchi et al. (2002). The Farquhar model was fitted to the data by applying iterative curve fitting (minimum least-square difference) using the Solver tool of Microsoft Excel.

Anatomical measurements

After the gas exchange measurements, transverse slices of 1×1 mm were cut between the main veins from the same leaves for anatomical measurements. Leaf material was quickly fixed under vacuum with 2% p-formaldehyde (2%) and glutaraldehyde (4%) in 0.1 M phosphate buffer solution (pH 7.2) and postfixed 1 h in 1% osmium tetroxide. Samples were dehydrated in (i) a graded ethanol series and (ii) propylene oxide and subsequently embedded in Embed-812 embedding medium (EMS, Hatfield, PA, USA). Semi-thin (0.8 μm) and ultrathin (90 nm) cross sections were cut with an ultramicrotome (Reichert & Jung model Ultracut E). Semi-thin cross sections were stained with 1% toluidine blue and viewed under a light microscopy (Optika B-600TiFL, Optika Microscopes, Ponteranica, Italy). Ultrathin cross sections were contrasted with uranyl acetate and lead citrate and viewed under a transmission electron microscope (TEM H600, Hitachi, Tokyo, Japan). Anatomical characteristics were derived from the micrographs with ImageJ software (http://rsb.info.nih.gov/nih-image/). Light microscopy images were used to determine the mesophyll thickness between the two epidermal layers (t_{mes}, μm), the fraction of the mesophyll tissue occupied by the intercellular air spaces (f_{ias}) (Patakas et al. 2003), and the mesophyll (S_m/S) and chloroplast (S_c/S) surface area facing intercellular air spaces per leaf area (Evans et al. 1994, Syvertsen et al. 1995, Tomás et al. 2013). All parameters were analyzed at least in four different fields of view and at three different sections. Electron microscopy images were used to determine the cell wall thickness (T_{cw}), cytoplasm thickness (T_{cyt}), chloroplast length (L_{chl}) and chloroplast thickness (T_{chl}) (Tomás et al. 2013). Three different sections and four to six different fields of view were used for measurements of each anatomical characteristic.

Mesophyll conductance modeled on the basis of anatomical characteristics

Leaf anatomical characteristics were used to estimate the g_m as a composite conductance for within-leaf gas and liquid components, according to the 1D gas diffusion model of Niinemets and Reichstein (2003) as applied by Tosens et al. (2012a):

$$g_m = \frac{1}{1/g_{ias} + (R \cdot T_k / H \cdot g_{liq})} \qquad (3)$$

where g_{ias} is the gas-phase conductance inside the leaf from substomatal cavities to outer surface of cell walls, g_{liq} is the conductance in liquid and lipid phases from outer surface of cell walls to chloroplasts, R is the gas constant (Pa m^3 K^{-1} mol^{-1}), T_k is the absolute temperature (K) and H is the Henry's law constant for CO_2 (Pa m^3 mol^{-1}). g_m is defined as a gas-phase conductance, and thus, $H/(RT_k)$, the dimensionless form of the Henry's law constant, is needed to convert g_{liq} to corresponding gas-phase equivalent conductance (Niinemets and Reichstein 2003).

The intercellular gas-phase conductance (and the reciprocal term, r_{ias}) was obtained according to Niinemets and Reichstein (2003) as:

$$g_{ias} = \frac{1}{r_{ias}} = \frac{D_A \cdot f_{ias}}{\Delta L_{ias} \cdot \tau} \qquad (4)$$

where ΔL_{ias} (m) is the average gas-phase thickness, τ is the diffusion path tortuosity (1.57 m m^{-1}, Syvertsen et al. 1995), D_A is the diffusivity of the CO_2 in the air (1.51 × 10^{-5} m^2 s^{-1} at 25 °C) and f_{ias} is the fraction of intercellular air spaces. ΔL_{ias} was taken as the half of the mesophyll thickness. Total liquid-phase conductance (g_{liq}) from the outer surface of cell walls to the carboxylation sites in the chloroplasts is the sum of serial conductances in the cell wall (r_{cw}), plasmalemma (r_{pl}) and inside the cell ($r_{cel,tot}$) (Tomás et al. 2013):

$$g_{liq} = \frac{S_m}{(r_{cw} + r_{pl} + r_{cel,tot}) \cdot S} \qquad (5)$$

The conductance of the cell wall was calculated as previously described in Peguero-Pina et al. (2012). For the conductance of plasma membrane, we used an estimate of 0.0035 m s^{-1} as previously suggested (Tosens et al. 2012a). The conductance inside the cell was calculated following the methodology described in Tomás et al. (2013), considering two different pathways of CO_2 inside the cell: one for cell wall parts lined with chloroplasts and the other for interchloroplastial areas (Tholen et al. 2012).

Analysis of partitioning changes in photosynthetic rate

The contribution analysis proposed by Buckley and Díaz-Espejo (2015) was used to partition changes in photosynthesis into contributions from the underlying variables. This new approach uses numerical integration having the advantage of avoiding the bias caused by discrete approximations like the widely used limitation analysis proposed by Grassi and Magnani (2005), and avoiding the need to compute partial derivatives for each variable. The method by Buckley and Díaz-Espejo (2015) relies instead on variable substitution in the photosynthesis model. This approach is easily extended to encompass effects of changes in any photosynthetic variable, under any conditions. Therefore, not only the contributions to photosynthesis in the Rubisco-limiting

region are represented now, but also those in the RuBP regeneration region.

Two analyses were performed. First, we compared *Q. robur* with *Q. faginea* to determine the main factor responsible for the lower A_N in the former species. Values in Table 4 were used to apply the contribution analysis. Second, we analyzed the effect of reduction in g_s (i.e., simulating a response to VPD or soil water deficit) in the % of contribution to A_N limitation. We assumed that, as g_s was reduced, g_m and $V_{c,max}$ were maintained constant.

Determination of total soluble protein, Rubisco and leaf nitrogen contents

Leaves from *Q. robur* and *Q. faginea* were ground in 500 µl of ice-cold extraction buffer containing 50 mM Bicine–NaOH (pH 8.0), 1 mM ethylenediaminetetracetic acid, 5% polyvinyl pyrrolidone, 6% polyethylene glycol (PEG$_{4000}$), 50 mM β-mercaptoethanol, 10 mM dithiothreitol and 1% protease-inhibitor cocktail (Sigma-Aldrich Co. LLC., USA). The extracts were centrifuged at 14,000g for 1 min at 4 °C and the total soluble protein (TSP) concentration in supernatant was quantified by the method of Bradford (1976). The concentration of Rubisco was determined with the gel electrophoresis method (Suárez et al. 2011, Bermúdez et al. 2012) using known concentrations of purified Rubisco from wheat as a standard for calibration.

Total leaf nitrogen (N) concentration was determined in dried leaves of *Q. robur* and *Q. faginea* using an Organic Elemental Analyzer (Flash EA 112, Thermo Fisher Scientific Inc., Waltham, MA, USA).

rbcL sequencing

Total genomic DNA from *Q. robur* and *Q. faginea* was isolated and purified using the DNeasy Plant Minikit (Qiagen, Hilden, Germany) following the manufacturer's instructions. The primers used for amplification and sequencing of the *rbc*L, the gene encoding the Rubisco large subunit, were esp2F (5′-ATGAGTT GTAGGGAGGGAC-3′) and 1494R (5′-GATTGGGCCGAGTTTA ATTTAC-3′) (Chen et al. 1998). Primers 414R (5′-CAAATCCTC CAGACGTAGAGC-3′) and 991R (5′-CGGTACCAGCGTGAATAT GAT-3′) (Chen et al. 1998) were also used only for sequencing. Polymerase chain reactions (PCRs) were performed in 50 µl using BioMix Red reagent mix (Bioline Ltd, London, UK). Polymerase chain reaction program for amplifications comprised initial cycle at 94 °C for 2 min, 55 °C for 30 s, 72 °C for 4 min, followed by 30 cycles of 94 °C for 30 s, 56 °C for 45 s and 72 °C for 1 min, and a final elongation at 72 °C for 5 min. The PCR products were separated on 2% agarose gels and purified using Roche High Pure PCR Product Purification Kit (Roche Diagnostics, Barcelona, Spain). The amplified PCR products were sequenced with an ABI 3100 Genetic analyzer using the ABI BigDye™ Terminator Cycle Sequencing Ready Reaction Kit (Applied Biosystems, Foster City, CA, USA).

Sequence chromatograms were checked and manually corrected and the contigs were assembled and aligned using MEGA 5.0 (Tamura et al. 2011).

Statistical analysis

Data are expressed as means ± standard error. Student's *t*-tests were used to compare the trait values between *Q. robur* and *Q. faginea*. All statistical analyses were carried out using SAS version 8.0 (SAS, Cary, NC, USA).

Results

The study of the morphological variables revealed an outstanding lower transpiring area in *Q. faginea* when compared with *Q. robur*, in terms of single leaf area, number of leaves, total leaf area per shoot and LAR (Table 2). In contrast, MVD and LMA were higher in *Q. faginea* (Table 2).

The hydraulic parameters of current-year twigs showed a sevenfold higher K_h in *Q. robur* when compared with *Q. faginea*. However, this difference in K_h between both species was buffered when expressed on a sapwood area basis (K_s) (Table 3), indicative of the production of conductive tissues with a similar efficiency in both species, or on a leaf area basis (LSC) (Table 3), explained by the higher investment in leaf area of *Q. robur*.

At ambient CO_2 concentration, 1.25 kPa of VPD and light-saturating intensity, A_N, E and g_s were higher in *Q. faginea* (19.6 µmol CO_2 m^{-2} s^{-1}, 6.5 mol H_2O m^{-2} s^{-1} and 0.652 mol H_2O m^{-2} s^{-1}, respectively) than in *Q. robur* (12.9 µmol CO_2 m^{-2} s^{-1}, 2.5 mol H_2O m^{-2} s^{-1} and 0.252 mol H_2O m^{-2} s^{-1}, respectively) (Table 4). Both the intrinsic (iWUE = A_N/g_s) and the instantaneous (WUE = A_N/E) water use efficiency were lower in *Q. faginea* (Table 4). The values of K_{leaf} for both species showed trends consistent with those described above for leaf gas exchange parameters: the value for *Q. faginea* (27.7 ± 1.5 mmol m^{-2} s^{-1} MPa^{-1}) was higher than that for *Q. robur* (17.9 ± 1.3 mmol m^{-2} s^{-1} MPa^{-1}) (Table 3). The differences in A_N were partly associated with the greater LMA in *Q. faginea* when compared with *Q. robur* (Table 2). In fact, when the net photosynthetic rate was expressed per unit dry mass, no statistically significant differences

Table 2. Leaf area, LMA, MVD, number of leaves per shoot, total leaf area per shoot and LAR for *Q. robur* and *Q. faginea*. Data are mean ± SE. Different letters indicate statistically significant differences ($P < 0.05$) between *Q. robur* and *Q. faginea*.

	Q. robur	*Q. faginea*
Leaf area (cm^2)	15.2 ± 1.4a	3.8 ± 0.2b
LMA (mg cm^{-2})	8.94 ± 1.30a	13.65 ± 0.65b
MVD (mm mm^{-2})	0.53 ± 0.02a	1.32 ± 0.03b
Number of leaves per shoot	11.2 ± 0.9a	7.5 ± 0.7b
Total leaf area per shoot (cm^2)	180 ± 26a	31 ± 4b
LAR (m^2 kg^{-1})	7.8 ± 0.2a	5.4 ± 0.1b

Table 3. K_h, K_s, LSC and K_{leaf} for *Q. robur* and *Q. faginea*. Data are mean ± SE. Different letters indicate statistically significant differences ($P < 0.05$) between *Q. robur* and *Q. faginea*.

	Q. robur	Q. faginea
K_h (kg m s^{-1} MPa^{-1})	$24.2 \times 10^{-7} \pm 7.2 \times 10^{-7}$a	$3.4 \times 10^{-7} \pm 0.9 \times 10^{-7}$b
K_s (kg m^{-1} s^{-1} MPa^{-1})	1.32 ± 0.28a	0.75 ± 0.14a
LSC (kg m^{-1} s^{-1} MPa^{-1})	$2.0 \times 10^{-4} \pm 3.2 \times 10^{-5}$a	$1.5 \times 10^{-4} \pm 4.0 \times 10^{-5}$a
K_{leaf} (mmol m^{-2} s^{-1} MPa^{-1})	17.9 ± 1.3a	27.7 ± 1.5b

Table 4. Mean values for the photosynthetic parameters analyzed at PPFD = 1500 μmol photons m^{-2} s^{-1}, T_{leaf} = 25 °C and VPD = 1.25 kPa. Data are mean ± SE. Different letters indicate statistically significant differences ($P < 0.05$) between *Q. robur* and *Q. faginea*. A_N, net photosynthesis; g_s, stomatal conductance; E, transpiration; iWUE = A_N/g_s, intrinsic water use efficiency; WUE = A_N/E, instantaneous water use efficiency; g_m, mesophyll conductance to CO_2; C_i, substomatal CO_2 concentration; C_c, chloroplastic CO_2 concentration; $V_{c,max}$ and J_{max}, maximum velocity of carboxylation and maximum capacity for electron transport; J_{flu}, electron transport rate estimated by chlorophyll fluorescence.

	Q. robur	Q. faginea
A_N (μmol CO_2 m^{-2} s^{-1})	12.9 ± 0.5a	19.6 ± 1.1b
g_s (mol H$_2$O m^{-2} s^{-1})	0.252 ± 0.013a	0.652 ± 0.078b
E (mol H$_2$O m^{-2} s^{-1})	2.5 ± 0.02a	6.5 ± 0.8b
iWUE (μmol mol^{-1})	51.2 ± 1.8a	31.7 ± 3.1b
WUE (μmol mol^{-1})	5.1 ± 0.3a	3.0 ± 0.2b
g_m (mol H$_2$O m^{-2} s^{-1})	0.060 ± 0.005a	0.098 ± 0.07b
C_i (μmmol CO_2 mol^{-1} air)	288 ± 7a	293 ± 4a
C_c (μmmol CO_2 mol^{-1} air)	80 ± 2a	95 ± 4b
$V_{c,max}$ (μmol m^{-2} s^{-1})	206 ± 6a	250 ± 4b
J_{max} (μmol m^{-2} s^{-1})	248 ± 10a	292 ± 14b
J_{flu} (μmol m^{-2} s^{-1})	266 ± 8a	306 ± 13b
$J_{max} : V_{c,max}$	1.21 ± 0.03a	1.19 ± 0.04a

Figure 2. Contributions of individual variables (g_s, stomatal conductance; g_m, mesophyll conductance to CO_2; $V_{c,max}$, maximum velocity of carboxylation) to the reduction in net CO_2 assimilation rate (A_N) shown by *Q. robur* using the values of *Q. faginea* as reference.

Figure 3. Contribution of stomatal conductance (g_s) to changes in net CO_2 assimilation rate (A_N) for *Q. robur* and *Q. faginea*.

($P < 0.05$) were found between *Q. robur* and *Q. faginea* (data not shown).

The mesophyll conductance to CO_2 (g_m) and the chloroplastic CO_2 concentration (C_c) were higher in *Q. faginea* (Table 4). Parameterization of the Farquhar et al. (1980) model of photosynthesis yielded higher values for $V_{c,max}$ and J_{max} in *Q. faginea*, although the ratio $J_{max} : V_{c,max}$ did not show differences between the two species (Table 4).

The analysis of the partitioning changes in photosynthesis revealed that A_N in *Q. robur* and *Q. faginea* was mainly limited by diffusional processes. Stomatal and, especially, mesophyll conductance limitations were responsible for the lower A_N measured in *Q. robur* in comparison with *Q. faginea* (Figure 2). *Quercus faginea* exhibited a large range of g_s, achieving values up to three times higher than *Q. robur*. As a consequence, a 50% reduction of g_s represents a A_N limitation of only 15% in *Q. faginea*; meanwhile, it means 35% for *Q. robur* (Figure 3). However, when comparing identical absolute values of g_s in both species, the A_N limitation due to stomata is always higher in *Q. faginea* than in *Q. robur* (Figure 3), greatly due to the higher $V_{c,max}$ in *Q. faginea* (Table 4).
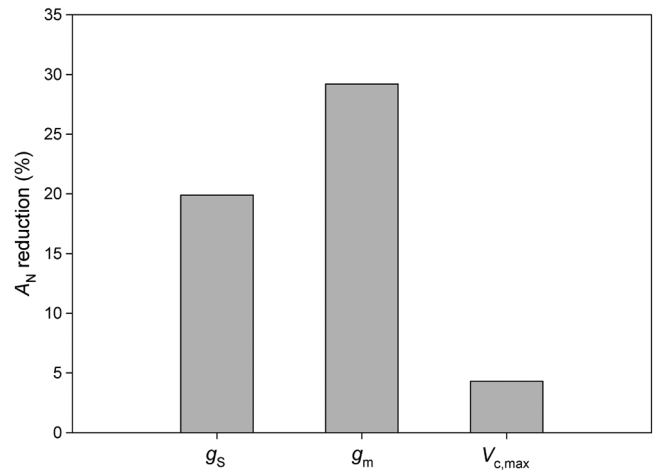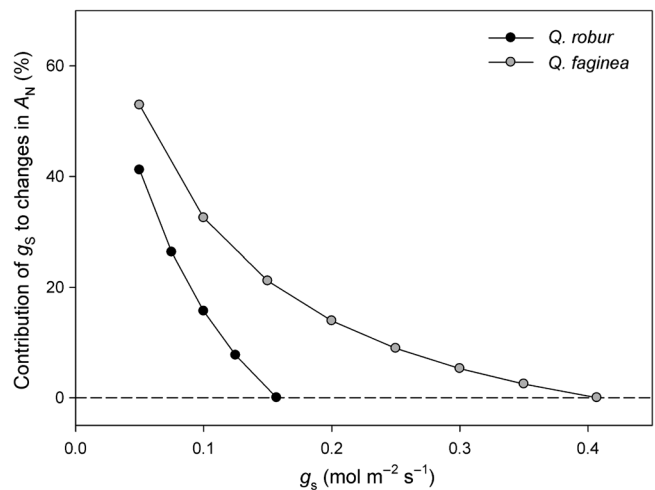
Quercus robur and *Q. faginea* displayed contrasting anatomical features at the leaf and cell levels. The mesophyll thickness, f_{ias}, S_m/S, S_c/S and S_c/S_m were higher in *Q. faginea*, while T_{cyt} and T_{chl} were higher in *Q. robur*, and no differences were found in T_{cw} and L_{chl} (Table 5). The anatomical parameters were further used to estimate different components of the CO_2 transfer resistances relative to total mesophyll resistance for both species (see

Table 5. Leaf type, mesophyll thickness, f_{ias}, mesophyll surface area exposed to intercellular airspace (S_m/S), chloroplast surface area exposed to intercellular airspace (S_c/S), the ratio S_c/S_m, T_{cw}, T_{cyt}, L_{chl} and T_{chl} in Q. robur and Q. faginea leaves. Data are mean ± SE. Different letters indicate statistically significant differences ($P < 0.05$) between Q. robur and Q. faginea.

	Q. robur	Q. faginea
Leaf type	Hypostomatous	Hypostomatous
Mesophyll thickness (μm)	140 ± 2a	186 ± 3b
f_{ias}	0.16 ± 0.01a	0.21 ± 0.01b
S_m/S (m^2 m^{-2})	21.9 ± 1.4a	28.4 ± 2.0b
S_c/S (m^2 m^{-2})	9.2 ± 1.0a	13.4 ± 1.7b
S_c/S_m	0.42 ± 0.02a	0.48 ± 0.02b
T_{cw} (μm)	0.262 ± 0.019a	0.270 ± 0.008a
T_{cyt} (μm)	0.109 ± 0.036a	0.026 ± 0.012b
L_{chl} (μm)	4.48 ± 0.29a	4.32 ± 0.16a
T_{chl} (μm)	1.87 ± 0.07a	1.21 ± 0.03b

Table 6. CO_2 transfer resistances across the intercellular air space (r_{ias}, s m^{-1}), the liquid phase (r_{liq}, s m^{-1}) and the mesophyll conductance for CO_2 (g_m, mol m^{-2} s^{-1}) calculated from anatomical measurements in Q. robur and Q. faginea. Data are mean ± SE. Different letters indicate statistically significant differences ($P < 0.05$) between Q. robur and Q. faginea.

	r_{ias} (s m^{-1})	r_{liq} (s m^{-1})	g_m (mol m^{-2} s^{-1})
Q. robur	46 ± 5a	391 ± 21a	0.091 ± 0.009a
Q. faginea	45 ± 6a	279 ± 18b	0.122 ± 0.008b

Table 7. Leaf N, TSP and Rubisco concentrations per leaf dry mass and per leaf area for Q. robur and Q. faginea. Data are mean ± SE. Different letters indicate statistically significant differences ($P < 0.05$) between Q. robur and Q. faginea.

	Q. robur	Q. faginea
g N/100 g	1.90 ± 0.15a	2.19 ± 0.18a
mol N m^{-2}	0.12 ± 0.02a	0.21 ± 0.03b
mg TSP g^{-1}	32.7 ± 1.4a	32.4 ± 0.4a
mg TSP m^{-2}	2922 ± 130a	4423 ± 55b
mg Rubisco/mg TSP	0.33 ± 0.01a	0.34 ± 0.01a
mg Rubisco g^{-1}	11.0 ± 0.5a	10.9 ± 0.3a
μmol Rubisco sites m^{-2}	17.6 ± 0.8a	26.7 ± 0.9b

Materials and methods for details). On one hand, regarding the gas phase, no differences were found in r_{ias} between both species (Table 6). On the other hand, regarding the liquid phase, the results demonstrated that Q. faginea presented lower values of r_{liq} than Q. robur (Table 6), which can be attributed to the lower values of T_{cyt} and T_{chl} found in Q. faginea (Table 5). Consequently, the estimated value of g_m was higher in Q. faginea than in Q. robur (Table 6), in agreement with the differences found in g_m obtained by gas exchange and chlorophyll fluorescence measurements (Table 4).

In Q. faginea, the concentration of N, TSP and Rubisco catalytic sites per leaf area were higher than in Q. robur (Table 7). The decreases in the concentration of TSP and Rubisco per leaf area in Q. robur with respect to Q. faginea were of similar magnitude, so that the ratio Rubisco/TSP was similar in both species (Table 7). Again, as stated above for A_N, when the concentration of N, TSP and Rubisco was expressed per unit dry mass, no differences ($P < 0.05$) were found between Q. robur and Q. faginea (Table 7).

Discussion

In this study, we have found a clear morphological and physiological segregation between Q. robur and Q. faginea, two 'roburoid oaks' occurring under contrasting climatic conditions (Table 1, Figure 1). The existence of a common ribulose-1,5-bisphosphate carboxylase/oxygenase (Rubisco) large subunit (rbcL) (see Figure S1 available as Supplementary Data at Tree Physiology Online) confirms the genetic proximity between these species, as stated in previous studies (Olalde et al. 2002, Himrane et al. 2004). Further, the identical rbcL sequence discards the existence of evolution trends in the 'quality' of Rubisco (i.e., related to different catalytic constants), in contrast with recent infrageneric comparative studies (Galmés et al. 2014a, 2014b). In spite of their genetic proximity, the two species constitute two very contrasting

functional types, showing a coordinated response at whole-plant level that would establish a differential physiological performance in response to climate dryness. Our results agree with recent studies that demonstrate strong interspecific correlations between hydraulic and photosynthetic traits (Brodribb et al. 2005, 2007, Sack and Holbrook 2006, Flexas et al. 2013).

Among all the studied traits, the differences found in leaf size constitute one of the most outstanding divergences between both species (Table 2). Thus, Q. faginea diminished the transpiring area, both in terms of single leaf area and number of leaves per shoot. Both traits imply a total leaf area per shoot about six times lower in Q. faginea than in Q. robur, with a direct consequence on the whole shoot transpiration in the former. A reduction in leaf size, such as that found in Q. faginea, has been proposed as one of the key traits that allows other Mediterranean oaks to withstand water deficit (Baldocchi and Xu 2007, Peguero-Pina et al. 2014). A direct benefit provided by small leaves is the improvement of the ability to supply water to transpiring leaves at shoot level in Q. faginea, offsetting the sharp difference found in K_h between both species (about seven times) for a similar K_s (Table 3). In this way, Q. faginea reached LSC values very similar to those measured for Q. robur (Table 3). An adjustment of LSC by reducing the whole-shoot leaf area has been previously reported by Peguero-Pina et al. (2014) in a comparison among Q. ilex provenances from contrasting climatic conditions. Another positive aspect of reducing leaf size in Q. faginea is the reduction of the aerodynamic resistance of leaves, which leads to a better coupling between leaf temperature and air temperature. This reduction in the aerodynamic resistance of leaves further enhances the control of transpiration by stomata (Jarvis and McNaughton 1986).

On the contrary, the reduction in the total leaf area per shoot had a negative impact on the carbon gain of *Q. faginea* and, through the effect on LAR, on its growth ability (Poorter and Remkes 1990). In this regard, *Q. faginea* presented several physiological traits that partially counteract the negative effects of leaf area reduction in terms of carbon assimilation. For instance, when compared with *Q. robur*, *Q. faginea* showed higher values for the main photosynthetic parameters (Table 4). Among them, it must be highlighted the extremely high values of g_s in *Q. faginea*. Such high values for g_s, which have been previously reported for this species (Acherar and Rambal 1992, Mediavilla and Escudero 2003, 2004), imply a high water consumption under the atmospheric evaporative demand experienced by this species during summer. The differences found in g_s between both species agreed with the differences found in K_{leaf} and MVD (Sack and Holbrook 2006, Sack and Scoffoni 2013), confirming the existence of a coordinated response between leaf hydraulics and gas exchange (Brodribb et al. 2007).

The maximum g_s values found in *Q. faginea* can be analyzed in the context of the stomatal sensitivity (i.e., the magnitude of the reduction in g_s with increasing VPD) reported by Mediavilla and Escudero (2003) for this species. According to the empirical model given by Oren et al. (1999), an exponential decrease in g_s would be expected as VPD increases, ranging from the values obtained at VPD close to 1 kPa to an expected value close to 0.220 mol H_2O m^{-2} s^{-1} at 3 kPa (Table 4, Figure 4a), which can be considered the maximum VPD expected value in the natural habitat of this species during the hottest period of the summer (Figure 1). The higher stomatal sensitivity of *Q. faginea* when compared with *Q. robur* is coherent with the higher $g_{s,max}$ measured in the former species (Oren et al. 1999) and implies the ability to cope with the higher VPD values experienced by *Q. faginea* through the vegetative period (Figure 1). In contrast, *Q. robur* showed a relatively low $g_{s,max}$ (as previously reported by Epron and Dreyer 1993, Rust and Roloff 2002, Arend et al. 2013) and, consequently, showed a lower stomatal sensitivity, which seems to be in accordance with the lower values of VPD registered through the vegetative period—below or close to 1 kPa—in its natural habitats (Figure 1). The transpiration values (*E*) calculated from the values of g_s for any VPD (Figure 4b) suggest that the differential stomatal sensitivity showed by *Q. robur* and *Q. faginea* keeps quite constant the *E* values for both species within the range of VPD values registered in their natural habitats (Figure 1).

The high $g_{s,max}$ value for *Q. faginea* found here and in previous studies (Acherar and Rambal 1992, Mediavilla and Escudero 2003, 2004) seems to be contradictory to the capacity of this species to live in Mediterranean areas. However, the high $g_{s,max}$ and the subsequent high stomatal sensitivity (Figure 4a) in *Q. faginea* in comparison with *Q. robur* must be interpreted taking into account the analysis of the stomatal limitations to the CO_2 photosynthetic assimilation (Figure 3). Effectively, the
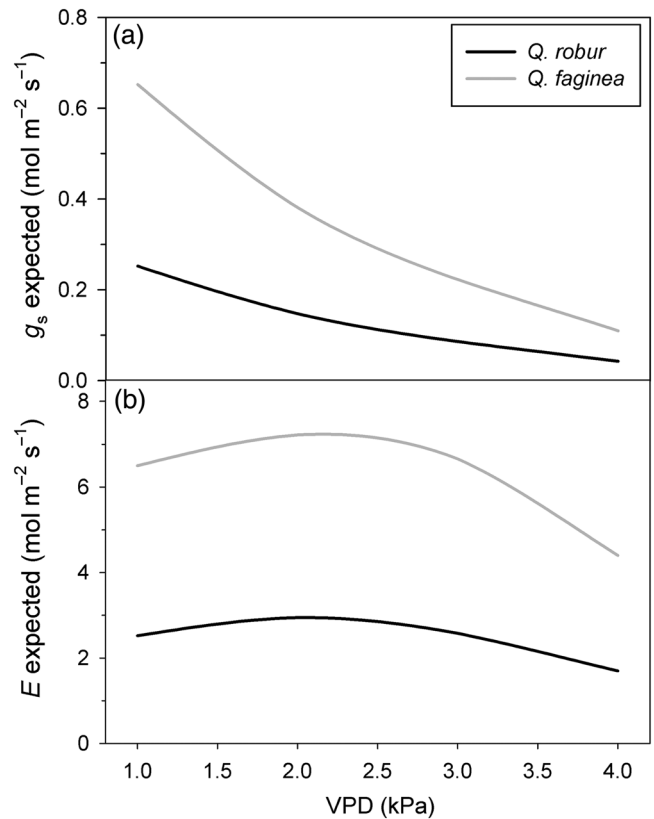

Figure 4. (a) Relationship between VPD and the expected stomatal conductance (g_s) and (b) relationship between VPD and the expected transpiration (*E*) for *Q. robur* and *Q. faginea* according to the empirical model given by Oren et al. (1999).

stomatal limitations to photosynthesis (A_N) in *Q. faginea* start at a g_s value of ~0.4 mol m^{-2} s^{-1}, which is expected to occur at a VPD value of ~2 kPa (Figure 4a). From this value, the contribution of g_s to the decrease in A_N (%) is progressively higher. However, at the maximum expected VPD value at midsummer (3 kPa, Figure 1), the expected contribution of g_s only diminished <20% of the maximum value of A_N at 1 kPa (Figure 3). In contrast, the curve predicting the contribution of g_s to changes in A_N (%) in *Q. robur* (Figure 3) shows a quite different shape, with a very sharp increase in the contribution of g_s to the decrease in A_N (%) once the stomatal regulation starts. In this sense, and under the climatic conditions experienced by *Q. faginea* (g_s <0.100 mol H_2O m^{-2} s^{-1} at 3 kPa), the stomatal limitations to photosynthesis in *Q. robur* will be higher than 30% (Figure 3). However, the absence of atmospheric dryness in the distribution range of *Q. robur* (Figure 1) allows this species to maintain stable photosynthetic rates along the vegetative period (Morecroft and Roberts 1999).

Contrary to *Q. robur*, the vegetative period in the distribution range of *Q. faginea* is affected by an important seasonality, expressed in terms of temperature, precipitation and VPD (Figure 1). Therefore, *Q. faginea* has to cope with a drop in the soil water content during summer that negatively affects the soil

water potential, consequently limiting the maximum values of g_s in this species (Acherar and Rambal 1992, Mediavilla and Escudero 2003, 2004). This double limitation to g_s, imposed by the stomatal sensitivity to VPD and to soil drought, may definitively limit the length of the vegetative period if the soil water reserves are depleted during the hottest and driest days of the summer. This may explain the extreme dependence of *Q. faginea* on edaphic conditions that ensure the maintenance of nonlimiting soil water potential values (Esteso-Martínez et al. 2006). In fact, different studies have evidenced the massive substitution of *Q. faginea* by the evergreen congeneric *Q. ilex* in most areas of the Iberian Peninsula as a consequence of the soil degradation associated with the human management of these areas (Corcuera et al. 2005a, 2005b).

On the other hand, the existence of a potential stress period during summer may be compensated by the prolongation of vegetative period along early- and mid-autumn, when temperature, water availability and VPD do not constrain the photosynthetic activity, as has been reported in several Mediterranean white oak species (Abadía et al. 1996, Mediavilla and Escudero 2003). Zhu et al. (2012) showed the strong dependence of vegetation phenology on latitude between 35°N and 70°N for North America, where a reduction in the length of the growing season of ~5 days per degree of latitude can be expected. The clearly southern distribution area of *Q. faginea* (from 35°N to 43°N) compared with *Q. robur* (40°N to ~60°N) (Jalas and Suominen 1976) should itself imply a longer vegetative period for the Mediterranean species, which may partially compensate for the severity of the environmental conditions in the middle of the growing season. According to this, Withington et al. (2006) found a leaf life span of 172 days (0.47 years) for *Q. robur* in central Poland at 51°N, while Mediavilla et al. (2001) reported a leaf life span of 208 days for *Q. faginea* (0.58 years) in central-western Spain at 41°N.

The higher inherent photosynthetic ability of *Q. faginea* when compared with *Q. robur* was not only a consequence of its higher $V_{c,max}$ but also relies on a higher g_m, which resulted in a higher chloroplastic CO_2 concentration (C_c) (Table 4). The differences in g_m between the two species can be partially attributed to the variation in leaf anatomical traits, i.e., T_{cyt} and T_{chl} (Table 5), that decreased r_{liq} in *Q. faginea* in comparison with *Q. robur* (Table 6). It should be noted that the role of anatomical traits in determining the specific variability in g_m has been previously reported in several studies (Tosens et al. 2012b, Tomás et al. 2013). In the present study, the g_m modeled based on leaf anatomical properties was higher than that estimated using conventional methods in *Q. robur* and *Q. faginea* (Tables 4 and 6). The reasons for such biases are not fully understood but are often observed in other studies (Peguero-Pina et al. 2012, Tomás et al. 2013, Carriquí et al. 2015). Nevertheless, the relative difference in g_m between the two species obtained with the two methods—gas exchange/fluorescence vs anatomical—

largely supports a predominant role of internal CO_2 diffusion in establishing photosynthetic differences between them.

The enhancement of all these functional traits in *Q. faginea* when compared with *Q. robur*—i.e., through the improvement of the instantaneous photosynthetic parameters—only partially counteract the negative effects of leaf area reduction in terms of carbon assimilation. Thus, taking into account the whole leaf area per shoot, *Q. robur* even shows an enhanced ability for carbon assimilation at whole-shoot level (data not shown), which results in a higher growth ability. On the other hand, the strong reduction in leaf area showed by *Q. faginea* would diminish the water losses at whole shoot level in comparison with *Q. robur* (data not shown), in spite of showing much higher g_s values (Table 4), which may be considered a key factor for withstanding the climate dryness imposed by the Mediterranean-type climates. However, in spite of the ability of *Q. faginea* to occupy most areas under Mediterranean climate (Olalde et al. 2002, Benito Garzón et al. 2008), the predictions indicate a notable reduction in its potential distribution range (Sánchez de Dios et al. 2009) as a consequence of the increment in aridity. Effectively, an increase in the length or in the intensity of summer drought will have a negative influence on the functional response of *Q. faginea* and other Mediterranean deciduous species (Gea-Izquierdo et al. 2013), as long as it would imply a shorter time period for carbon assimilation and a lower productivity (Gea-Izquierdo and Cañellas 2014). Under these conditions, evergreen oaks—such as *Q. ilex*—can obtain a benefit from their more 'conservative' leaf strategy (Wright et al. 2004) that allows the use of other periods through the year, such as the early spring or late autumn (Corcuera et al. 2005a).

Conclusions

Quercus faginea can be regarded as an example of adaptation of a deciduous oak to the Mediterranean-type climates, as fossil records indicate (Roiron 1983, Barrón et al. 2010). In our opinion, the reduction in transpiring area both at leaf and shoot level in *Q. faginea*, when compared with the mesic-temperate *Q. robur*, is the main trait imposed by the water deficit in Mediterranean-type climates. The reduction in LAR in *Q. faginea* should have a negative effect of carbon gain that is partially compensated with a higher A_N at the expense of a much higher maximum g_s, which has been considered one key trait for classifying this species as a 'water spender' (Mediavilla and Escudero 2004). We propose that the extremely high g_s values in *Q. faginea* counteract the reduction in g_s imposed by the stomatal sensitivity to VPD, allowing this species to maintain high A_N values through the changing conditions along the vegetative period in its natural habitat. The depletion of soil water reserves at midsummer should impose a further limitation in the vegetative activity of this species, which explain its substitution by other species (e.g., *Q. ilex*) in

degraded soils and can also explain the extreme vulnerability of this species to an increment in aridity associated with a global climatic change (Sánchez de Dios et al. 2009).

Supplementary data

Supplementary data for this article are available at *Tree Physiology* Online.

Acknowledgments

Conflict of interest

None declared.

Funding

References

Abadía A, Gil E, Morales F, Montañés L, Montserrat G, Abadía J (1996) Marcescence and senescence in a submediterranean oak (*Quercus subpyrenaica* E.H. del Villar): photosynthetic characteristics and nutrient composition. Plant Cell Environ 19:685–694.

Acherar M, Rambal S (1992) Comparative water relations of four Mediterranean oak species. Vegetatio 99–100:177–184.

Arend M, Brem A, Kuster TM, Günthardt-Goerg MS (2013) Seasonal photosynthetic responses of European oaks to drought and elevated daytime temperature. Plant Biol 15:169–176.

Axelrod DI (1983) Biogeography of oaks in the Arcto-Tertiary province. Ann Mo Bot Gard 70:629–657.

Baldocchi DD, Xu L (2007) What limits evaporation from Mediterranean oak woodlands—the supply of moisture in the soil, physiological control by plants or the demand by the atmosphere? Adv Water Resour 30:2113–2122.

Barrón E, Rivas-Carballo R, Postigo-Mijarra JM, Alcalde-Olivares C, Vieira M, Castro L, Pais J, Valle-Hernández M (2010) The Cenozoic vegetation of the Iberian Peninsula: a synthesis. Rev Palaeobot Palynol 162:382–402.

Benito Garzón M, Sánchez de Dios R, Sáinz Ollero H (2007) Predictive modelling of tree species distributions on the Iberian Peninsula during the Last Glacial Maximum and Mid-Holocene. Ecography 30:120–134.

Benito Garzón M, Sánchez de Dios R, Sainz Ollero H (2008) Effects of climate change on the distribution of Iberian tree species. Appl Veg Sci 11:169–178.

Bermúdez MA, Galmés J, Moreno I, Mullineaux PM, Gotor C, Romero LC (2012) Photosynthetic adaptation to length of day is dependent on S-sulfocysteine synthase activity in the thylakoid lumen. Plant Physiol 160:274–288.

Bernacchi CJ, Portis AR, Nakano H, von Caemmerer S, Long SP (2002) Temperature response of mesophyll conductance. Implications for the determination of Rubisco enzyme kinetics and for limitations to photosynthesis in vivo. Plant Physiol 130:1992–1998.

Bradford MM (1976) A rapid and sensitive method for the quantitation of microgram quantities of protein utilizing the principle of protein-dye binding. Anal Biochem 72:248–254.

Brodribb TJ, Holbrook NM (2004) Diurnal depression of leaf hydraulic conductance in a tropical tree species. Plant Cell Environ 27:820–827.

Brodribb TJ, Holbrook NM, Zwieniecki MA, Palma B (2005) Leaf hydraulic capacity in ferns, conifers and angiosperms: impacts on photosynthetic maxima. New Phytol 165:839–846.

Brodribb TJ, Field TS, Jordan GJ (2007) Leaf maximum photosynthetic rate and venation are linked by hydraulics. Plant Physiol 144:1890–1898.

Buckley TN, Díaz-Espejo A (2015) Partitioning changes in photosynthetic rate into contributions from different variables. Plant Cell Environ 38:1200–1211.

Carriquí M, Cabrera HM, Conesa MÀ et al. (2015) Diffusional limitations explain the lower photosynthetic capacity of ferns as compared with angiosperms in a common garden study. Plant Cell Environ 38:448–460.

Chen ZD, Wang XQ, Sun HY, Han Y, Zhang ZX, Zou YP, Lu AM (1998) Systematic position of the Rhoipteleaceae: evidence from nucleotide sequences of rbcL gene. Acta Phytotaxon Sin 36:1–7.

Corcuera L, Camarero JJ, Gil-Pelegrín E (2002) Functional groups in *Quercus* species derived from the analysis of pressure-volume curves. Trees 16:465–472.

Corcuera L, Camarero JJ, Gil-Pelegrín E (2004) Effects of a severe drought on growth and wood anatomical properties of *Quercus faginea*. IAWA J 25:185–204.

Corcuera L, Morales F, Abadía A, Gil-Pelegrín E (2005*a*) Seasonal changes in photosynthesis and photoprotection in a *Quercus ilex* subsp. *ballota* woodland located in its upper altitudinal extreme in the Iberian Peninsula. Tree Physiol 25:599–608.

Corcuera L, Morales F, Abadía A, Gil-Pelegrín E (2005*b*) The effect of low temperatures on the photosynthetic apparatus of *Quercus ilex* subsp. *ballota* at its lower and upper altitudinal limits in the Iberian Peninsula and during a single freezing-thawing cycle. Trees 19:99–108.

Denk T, Grimm GW (2009) Significance of pollen characteristics for infrageneric classification and phylogeny in *Quercus* (Fagaceae). Int J Plant Sci 170:926–940.

Denk T, Grimm GW (2010) The oaks of western Eurasia: traditional classifications and evidence from two nuclear markers. Taxon 59:351–366.

Ducousso A, Bordacs S (2004) EUFORGEN Technical Guidelines for genetic conservation and use for pedunculate and sessile oaks (*Quercus robur* and *Q. petraea*). International Plant Genetic Resources Institute, Rome, Italy, 6 pp.

Epron D, Dreyer E (1993) Long-term effects of drought on photosynthesis of adult oak trees [*Quercus petraea* (Matt.) Liebl. and *Quercus robur* L.] in a natural stand. New Phytol 125:381–389.

Esteso-Martínez J, Camarero JJ, Gil-Pelegrín E (2006) Competitive effects of herbs on *Quercus faginea* seedlings inferred from vulnerability curves and spatial-pattern analyses in a Mediterranean stand (Iberian System, northeast Spain). Ecoscience 131:378–387.

Evans JR, von Caemmerer S, Setchell BA, Hudson GS (1994) The relationship between CO₂ transfer conductance and leaf anatomy in transgenic tobacco with a reduced content of Rubisco. Aust J Plant Physiol 21:475–495.

Farquhar GD, von Caemmerer S, Berry JA (1980) A biochemical model of photosynthetic CO₂ assimilation in leaves of C₃ species. Planta 149:78–90.

Flexas J, Díaz-Espejo A, Berry JA, Galmés J, Cifre J, Kaldenhoff R, Medrano H, Ribas-Carbó M (2007*a*) Analysis of leakage in IRGA's leaf chambers

of open gas exchange systems: quantification and its effects in photosynthesis parameterization. J Exp Bot 58:1533–1543.

Flexas J, Ortuño MF, Ribas-Carbó M, Díaz-Espejo A, Flórez-Sarasa ID, Medrano H (2007b) Mesophyll conductance to CO_2 in *Arabidopsis thaliana*. New Phytol 175:501–511.

Flexas J, Scoffoni C, Gago J, Sack L (2013) Leaf mesophyll conductance and leaf hydraulic conductance: an introduction to their measurement and coordination. J Exp Bot 64:3965–3981.

Galmés J, Andralojc PJ, Kapralov MV, Flexas J, Keys AJ, Molins A, Parry MAJ, Conesa MÀ (2014a) Environmentally driven evolution of Rubisco and improved photosynthesis and growth within the C_3 genus *Limonium* (Plumbaginaceae). New Phytol 203:989–999.

Galmés J, Kapralov MV, Andralojc PJ, Conesa MÀ, Keys AJ, Parry MAJ, Flexas J (2014b) Expanding knowledge of the Rubisco kinetics variability in plant species: environmental and evolutionary trends. Plant Cell Environ 37:1989–2001.

Gea-Izquierdo G, Cañellas I (2014) Local climate forces instability in long-term productivity of a Mediterranean oak along climatic gradients. Ecosystems 17:228–241.

Gea-Izquierdo G, Fernández-de-Uña L, Cañellas I (2013) Growth projections reveal local vulnerability of Mediterranean oaks with rising temperatures. For Ecol Manag 305:282–293.

Genty B, Briantais JM, Baker NR (1989) The relationship between the quantum yield of photosynthetic electron transport and quenching of chlorophyll fluorescence. Biochim Biophys Acta 990:87–92.

Grassi G, Magnani F (2005) Stomatal, mesophyll conductance and biochemical limitations to photosynthesis as affected by drought and leaf ontogeny in ash and oak trees. Plant Cell Environ 28:834–849.

Harley PC, Loreto F, Di Marco G, Sharkey TD (1992) Theoretical considerations when estimating the mesophyll conductance to CO_2 flux by analysis of the response of photosynthesis to CO_2. Plant Physiol 98:1429–1436.

Himrane H, Camarero JJ, Gil-Pelegrín E (2004) Morphological and ecophysiological variation of the hybrid oak *Quercus subpyrenaica* (*Q. faginea × Q. pubescens*). Trees 18:566–575.

Jalas J, Suominen J (eds) (1976) Atlas Florae Europaeae. Distribution of vascular plants in Europe. 3. Salicaceae to Balanophoraceae. The Committee for Mapping the Flora of Europe & Societas Biologica Fennica Vanamo, Helsinki, 128 pp. [maps 201–383].

Jarvis PG, McNaughton KG (1986) Stomatal control of transpiration: scaling up from leaf to region. Adv Ecol Res 15:1–49.

Jato V, Rodríguez-Rajo FJ, Méndez J, Aira MJ (2002) Phenological behaviour of *Quercus* in Ourense (NW Spain) and its relationship with the atmospheric pollen season. Int J Biometeorol 46:176–184.

Kikuzawa K (1995) Leaf phenology as an optimal strategy for carbon gain in plants. Can J Bot 73:158–163.

Kovar-Eder J, Kvacek Z, Zastawniak E, Givulescu R, Hably L, Mihajlovic D, Teslenko Y, Walther H (1996) Floristic trends in the vegetation of the Paratethys surrounding areas during Neogene time. In: Bernor R, Fahlbusch V, Mittmann HW (eds) The evolution of Western Eurasia Later Neogene faunas. Columbia University Press, New York, pp 399–409.

Krall JP, Edwards GE (1992) Relationship between photosystem II activity and CO_2 fixation in leaves. Physiol Plant 86:180–187.

Kremer A, Abbott AG, Carlson JE, Manos PS, Plomion C, Sisco P, Staton ME, Ueno S, Vendramin GG (2012) Genomics of Fagaceae. Tree Genet Genomes 8:583–610.

Kvacek Z, Walther H (1989) Palaeobotanical studies in Fagaceae of the European Tertiart. Plant Syst Evol 162:213–229.

Laisk AK (1977) Kinetics of photosynthesis and photorespiration in C_3-plants. Nauka, Moscow, Russia (In Russian).

Manos PS, Doyle JJ, Nixon KC (1999) Phylogeny, biogeography, and processes of molecular differentiation in *Quercus* subgenus *Quercus* (Fagaceae). Mol Phylogenet Evol 12:333–349.

Mayr S, Wieser G, Bauer H (2006) Xylem temperatures during winter in conifers at the alpine timberline. Agric For Meteorol 137:81–88.

Mediavilla S, Escudero A (2003) Stomatal responses to drought at a Mediterranean site: a comparative study of co-occurring woody species differing in leaf longevity. Tree Physiol 23:987–996.

Mediavilla S, Escudero A (2004) Stomatal responses to drought of mature trees and seedlings of two co-occurring Mediterranean oaks. For Ecol Manag 187:281–294.

Mediavilla S, Escudero A, Heilmeier H (2001) Internal leaf anatomy and photosynthetic resource-use efficiency: interspecific and intraspecific comparisons. Tree Physiol 21:251–259.

Morecroft MD, Roberts JM (1999) Photosynthesis and stomatal conductance of mature canopy Oak (*Quercus robur*) and Sycamore (*Acer pseudoplatanus*) trees throughout the growing season. Funct Ecol 13:332–342.

Niinemets Ü, Reichstein M (2003) Controls on the emission of plant volatiles through stomata: a sensitivity analysis. J Geophys Res 108:4211. doi:10.1029/2002JD002626

Ogaya R, Peñuelas J (2007) Leaf mass per area ratio in *Quercus ilex* leaves under a wide range of climatic conditions. The importance of low temperatures. Acta Oecol 31:168–173.

Olalde M, Herrán A, Espinel S, Goicoechea PG (2002) White oaks phylogeography in the Iberian Peninsula. For Ecol Manag 156:89–102.

Oren R, Sperry JS, Katul GG, Pataki DE, Ewers BE, Phillips N, Schäfer KVR (1999) Survey and synthesis of intra- and interspecific variation in stomatal sensitivity to vapour pressure deficit. Plant Cell Environ 22:1515–1526.

Patakas A, Kofidis G, Bosabalidis AM (2003) The relationships between CO_2 transfer mesophyll resistance and photosynthetic efficiency in grapevine cultivars. Sci Hortic 97:255–263.

Peguero-Pina JJ, Flexas J, Galmés J, Niinemets Ü, Sancho-Knapik D, Barredo G, Villarroya D, Gil-Pelegrín E (2012) Leaf anatomical properties in relation to differences in mesophyll conductance to CO_2 and photosynthesis in two related Mediterranean *Abies* species. Plant Cell Environ 35:2121–2129.

Peguero-Pina JJ, Sancho-Knapik D, Barrón E, Camarero JJ, Vilagrosa A, Gil-Pelegrín E (2014) Morphological and physiological divergences within *Quercus ilex* support the existence of different ecotypes depending on climatic dryness. Ann Bot 114:301–313.

Piedallu C, Gégout JC, Perez V, Lebourgeois F (2013) Soil water balance performs better than climatic water variables in tree species distribution modelling. Glob Ecol Biogeogr 22:470–482.

Poorter H, Remkes C (1990) Leaf area ratio and net assimilation rate of 24 wild species differing in relative growth rate. Oecologia 83:553–559.

Roiron P (1983) Nouvelle étude de la macroflore plio-pléistocène de Crespià (Catalogne, Espagne). Geobios 16:687–715.

Rust S, Roloff A (2002) Reduced photosynthesis in old oak (*Quercus robur*): the impact of crown and hydraulic architecture. Tree Physiol 22:597–601.

Sack L, Holbrook NM (2006) Leaf hydraulics. Annu Rev Plant Biol 57:361–381.

Sack L, Scoffoni C (2013) Leaf venation: structure, function, development, evolution, ecology and applications in the past, present and future. New Phytol 198:983–1000.

Sánchez de Dios R, Benito-Garzón M, Sainz-Ollero H (2009) Present and future extension of the Iberian submediterranean territories as determined from the distribution of marcescent oaks. Plant Ecol 204:189–205.

Scoffoni C, Rawls M, McKown A, Cochard H, Sack L (2011) Decline of leaf hydraulic conductance with dehydration: relationship to leaf size and venation architecture. Plant Physiol 156:832–843.

Suárez R, Miró M, Cerdà V, Perdomo JA, Galmés J (2011) Automated flow-based anion-exchange method for high-throughput isolation and real-time monitoring of RuBisCO in plant extracts. Talanta 84:1259–1266.

Syvertsen JP, Lloyd J, McConchie C, Kriedemann PE, Farquhar GD (1995) On the relationship between leaf anatomy and CO_2 diffusion through the mesophyll of hypostomatous leaves. Plant Cell Environ 18:149–157.

Tamura K, Peterson D, Peterson N, Stecher G, Nei M, Kumar S (2011) MEGA5: molecular evolutionary genetics analysis using maximum likelihood, evolutionary distance, and maximum parsimony methods. Mol Biol Evol 28:2731–2739.

Tholen D, Ethier G, Genty B, Pepin S, Zhu X (2012) Variable mesophyll conductance revisited: theoretical background and experimental implications. Plant Cell Environ 35:2087–2103.

Tomás M, Flexas J, Copolovici L et al. (2013) Importance of leaf anatomy in determining mesophyll diffusion conductance to CO_2 across species: quantitative limitations and scaling up by models. J Exp Bot 64:2269–2281.

Tosens T, Niinemets Ü, Vislap V, Eichelmann H, Castro Díez P (2012a) Developmental changes in mesophyll diffusion conductance and photosynthetic capacity under different light and water availabilities in *Populus tremula*: how structure constrains function. Plant Cell Environ 35:839–856.

Tosens T, Niinemets Ü, Westoby M, Wright IJ (2012b) Anatomical basis of variation in mesophyll resistance in eastern Australian sclerophylls: news of a long and winding path. J Exp Bot 63:5105–5119.

Valentini R, Epron D, De Angelis P, Matteucci G, Dreyer E (1995) In situ estimation of net CO_2 assimilation, photosynthetic electron flow and photorespiration in Turkey oak (*Q. cerris* L.) leaves: diurnal cycles under different levels of water supply. Plant Cell Environ 18:631–640.

van Ommen Kloeke AEE, Douma JC, Ordoñez JC, Reich PB, van Bodegom PM (2012) Global quantification of contrasting leaf life span strategies for deciduous and evergreen species in response to environmental conditions. Glob Ecol Biogeogr 21:224–235.

Vilagrosa A, Bellot J, Vallejo VR, Gil-Pelegrín E (2003) Cavitation, stomatal conductance, and leaf dieback in seedlings of two co-occurring Mediterranean shrubs during an intense drought. J Exp Bot 54:2015–2024.

Withington JM, Reich PB, Oleksyn J, Eissenstat DM (2006) Comparisons of structure and life span in roots and leaves among temperate trees. Ecol Monogr 76:381–397.

Wright IJ, Reich PB, Westoby M et al. (2004) The worldwide leaf economics spectrum. Nature 428:821–827.

Zhu W, Tian H, Xu X, Pan Y, Chen G, Lin W (2012) Extension of the growing season due to delayed autumn over mid and high latitudes in North America during 1982–2006. Glob Ecol Biogeogr 21:260–271.